Inorganic Chemistry

Article

pubs.acs.org/IC

Selective Binding of Zn^{2+} Complexes to Human Telomeric G-Quadruplex DNA

Kevin E. Siters,[†] Matthew A. Fountain,*[,‡] and Janet R. Morrow*[,†]

[†]Department of Chemistry, University at Buffalo, State University of New York, Buffalo, New York 14260, United States

[‡]Department of Chemistry and Biochemistry, State University of New York, College at Fredonia, Fredonia, New York 14063, United States

Supporting Information

ABSTRACT: The Zn^{2+} complex of 5-(1,4,7,10-tetraazacyclododecan-1-ylsulfonyl)-*N*,*N*-dimethylnaphthalen-1-amine, Zn(DSC), binds selectively to the biologically relevant human telomeric (H-Telo) G-quadruplex. An increase in the Zn(DSC) dansyl group fluorescence with a simultaneous shift in emission is consistent with the complex binding to H-Telo. The H-Telo G-quadruplex has two binding sites for Zn(DSC) with binding constants in the low micromolar range (2.5 μM). Isothermal calorimetric titrations confirm low micromolar dissociation constants with a 2:1 stoichiometry. The interaction between H-Telo and Zn(DSC) is highly pH-dependent, consistent with binding to the unpaired thymines in the G-quadruplex loops. As a result, Zn(DSC) selectively binds to H-Telo over duplex DNA. In contrast to Zn^{2+}, Fe^{2+} and Co^{2+} do not complex to the DSC macrocycle appreciably under the conditions of the experiment. The Cu^{2+} complex of DSC does not interact measurably with the H-Telo G-quadruplex. Interestingly, the H-Telo-Zn(DSC) adduct self-assembles from its individual components at physiological pH and 100 mM KCl. The self-assembly feature, which is specific for the Zn^{2+} ion, suggests that this system may be viable as a Zn^{2+} sensor. Pentanucleotides were studied in order to better describe the binding of Zn(DSC) to thymine sequences. NMR studies were consistent with the binding of Zn(DSC) to thymine-containing oligonucleotides including CCTCC, CTTCC, and CTCTC. Studies showed that the dansyl group of Zn(DSC) interacts with thymines in CTTCC. Fluorescence spectroscopy and ITC data indicate that Zn(DSC) forms 2:1 adducts with thymines that are spaced (CTCTC) but not tandem thymines (CTTCC). These data are consistent with one Zn(DSC) complex binding to two separate loops in the G-quadruplex. A second Zn^{2+} complex containing an acridine pendent, Zn(ACR), binds tightly to pentanucleotides with both tandem and spaced thymines. Zn(ACR) indiscriminately binds to both H-Telo and duplex DNA.

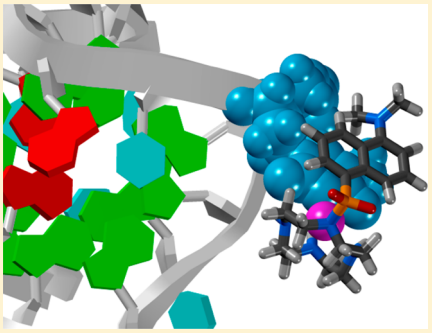

INTRODUCTION

The design of metal-ion complexes for targeting nucleic acid structures is of long-standing interest to inorganic chemists.[1−3] One nucleic acid structure that is currently the focus of many studies is formed in the telomeric region of chromosomes that contain tandem repeats of guanine-rich sequences for folding into G-quadruplex structures.[4−7] These higher-order secondary structures feature four guanines interacting through Hoogsteen hydrogen bonding to give a planar structure called a G-tetrad. Most biologically relevant G-quadruplexes are formed in an intramolecular fashion such that the guanine tracts form G-tetrads that are connected through a series of loops. The G-quadruplexes are characterized, in part, by the directionality of the strands being parallel or antiparallel or by hybrid structures that contain both parallel and antiparallel nucleic acid strands. In particular, the human telomeric G-quadruplex [H-Telo: 5′-$A(GGGTTA)_3$-3′] generally forms a hybrid topology in solutions containing K^+, the predominant alkali-metal ion inside cells,[8,9] but a parallel topology in solutions containing high sodium ion concentrations (Figure 1).[10−12] Such G-quadruplexes are of interest because regulation of telomeres impacts the duration of cell life through genomic stability. In normal cells, telomerase is expressed in transient levels and may enable regulation of the cell lifespan.[13] In cancer cells, telomeres are maintained as a result of upregulated telomerase levels.[14] Small-molecule recognition of G-quadruplexes is currently of interest in view of the growing importance of these structures in nucleic acid regulation.[5] The role of telomeric extension in cancer has generated interest in the stabilization of the human telomeric G-quadruplex as a

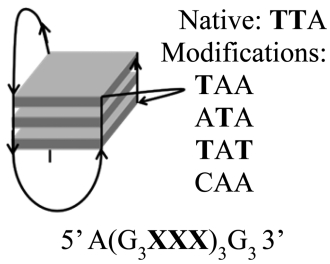

Figure 1. H-Telo 3 + 1 topology, including loop sequences.

Received: June 27, 2014
Published: October 13, 2014

potential anticancer target.[6] For example, molecules that selectively bind to and stabilize the G-quadruplexes in the telomeric regions may interfere in the upregulation of telomere extension, a potentially important process in cancer cell immortality. However, it is challenging to design a molecule that selectively binds to G-quadruplex DNA over duplex DNA.

One important class of G-quadruplex ligands consists of large heterocycles that exhibit nanomolar binding to H-Telo.[15−20] These ligands generally rely on hydrophobic interactions between the G-tetrad and ligand.[21] Cationic organic side chains are frequently used to help stabilize the G-quadruplex by interacting with the surrounding loops; however, these interactions are generally of secondary importance.[22,23] Neidle et al. designed a trisubstituted acridine that stacks on the G-tetrad in one particularly successful approach for inhibiting upregulated telomerase action: BRACO-19.[24,25] X-ray crystal structures show a parallel G-quadruplex with cationic pyrrolidine and dimethylaniline groups interacting with surrounding water molecules and the negatively charged phosphate backbone of the DNA.[22] Other molecules such as telomestatin were shown to inhibit telomerase activity,[26] while exhibiting selectivity over duplex DNA.[27] Telomestatin was shown to form a 2:1 adduct with the antiparallel, or basket, conformation of H-Telo[28] and can interconvert H-Telo from a 3 + 1 topology to basket topology in K^+ solutions.[29] Similar cationic porphyrins such as TMPyP4 were shown to inhibit telomerase at low micromolar concentrations but show poor selectivity toward duplex DNA.[19,30,31] Selectivity is improved with the use of transition-metal-ion complexes, such as Mn^{2+} porphyrins.[32,33]

Metal coordination complexes have been developed for selective recognition of G-quadruplexes. For example, a Ni^{2+}-salphen complex stabilizes H-Telo through end stacking on the G-quartet.[34] Variation of the transition metal and alteration of the geometry of the complex can greatly affect binding to H-Telo.[35,36] Moreover, retaining a square-planar geometry of the complex has been shown to be imperative for tight binding to H-Telo.[37,38] Similar complexes have been developed using Pd^{2+} and Pt^{2+} metal ions that feature a flat, large aromatic surface area, which is ideal for stacking on the G-tetrad.[39,40] These complexes, like their organic counterparts, rely on generating a large aromatic surface area for $\pi-\pi$ stacking with the G-tetrad. The metal ion is largely used for spatial arrangement of the aromatic substituents in a square-planar geometry and does not directly interact with the G-quadruplex. The reader is directed to these reviews for a comprehensive treatment of the interaction of coordination complexes with G-quadruplexes.[3,7]

G-quadruplexes have also been utilized to facilitate metal-ion sensing. For example, H-Telo, with the assistance of an external fluorophore, exhibits selectivity as a K^+ ion sensor. In a study by the Zhang group, the K^+ ion induces the folding of H-Telo into the hybrid 3 + 1 conformation and allows for the selective binding of thioflavin to the G-tetrad, eliciting a fluorescent response.[41] In Na^+ solutions, G-quadruplexes form a basket conformation and cannot bind thioflavin. This fluorescence response was selective for K^+ over analogous metals and transition metals. Similarly, Wang et al. developed a sensor selective for K^+, using a native C-myc G-quadruplex.[42] Disrupting the G-quadruplex secondary structure has been utilized in sensing Hg^{2+}. In this example, a G-quadruplex−thioflavin adduct is disrupted by Hg^{2+} to produce a decrease in thioflavin fluorescence.[43] A comprehensive review on using G-quadruplexes as sensors has been recently published.[44]

Herein we propose a previously unreported mode of G-quadruplex recognition that involves thymine loop recognition by Zn^{2+} macrocyclic complexes. Recognition of thymine nucleobases by Zn^{2+} macrocyclic complexes has been studied extensively by the Kimura group,[45] although predominantly in single-stranded DNA. Zn^{2+} macrocyclic complexes interact with thymine- or uracil-containing nucleic acids through binding to the deprotonated N3 site of the pyrimidine ring ($N3^-$).[46,47] In order for the Zn^{2+} complex to bind in this manner, the thymine or uracil groups must be in a noncannonical context so that their Watson−Crick face is accessible and not involved in base pairing. Kimura and co-workers studied the binding of mononuclear and dinuclear Zn^{2+} complexes to single-stranded nucleic acids.[48] Kimura's group also found that Zn^{2+} complexes with large aromatic pendents, such as acridine, bound to double-stranded DNA or RNA.[49] Duplex stabilization or denaturation in the presence of these complexes was sequence-dependent.[48,50] While most reports from the Kimura group featured the cyclen macrocycle, our group and others have shown that a variety of macrocyclic complexes of Zn^{2+} bind to thymine or uracil groups.[51−57]

Zn^{2+} macrocyclic complexes with aromatic pendent groups are bifunctional recognition agents that can be tuned to bind to thymine or uracil groups in different structural contexts.[45,51,54,56,57] Zn^{2+} complex binding to $N3^-$ of thymine is modulated, in part, by the Lewis acidity of the Zn^{2+} center, which can be varied by the choice of the macrocycle.[52] The aromatic pendent group further influences recognition by stacking on the thymine or, if there are two bound Zn^{2+} complexes on adjacent thymines, by stacking on itself.[49,58] Alternatively, pendents may interact with other nucleotides within the DNA structure.[50,57] The combination of variable Zn^{2+} coordination and variable aromatic pendents can be used to tune the selectivity of the complex toward different nucleic acid structures.[47] For example, our work has shown that Zn^{2+} macrocyclic complexes with planar heteroatom-containing pendent groups bind strongly to thymine bulges, whereas Zn^{2+} complexes with nonplanar pendents such as Zn(DSC) do not.[57] Zn(DSC) has been shown to bind to single-stranded oligonucleotides as well as duplexes containing abasic sites with an adjacent thymine.[51]

Here we show that Zn(DSC) binds selectively to the H-Telo G-quadruplex structure found in human DNA, which contains thymines in three different loops. The complex also binds to single-stranded oligonucleotides containing thymines in similar sequences, allowing for characterization of binding and determination of stoichiometry. Zn(DSC) has a nonplanar pendent dansyl group, which does not favor intercalation. For comparison, Zn(ACR), which contains a pendent acridine group that is often used for G-quadruplex tetrad recognition, was studied as a recognition agent for the H-Telo G-quadruplex (Figure 2).

EXPERIMENTAL METHODS

The macrocycle 5-(1,4,7,10-tetraazacyclododecan-1-ylsulfonyl)-*N*,*N*-dimethylnaphthalen-1-amine (DSC) and complex $[Zn(DSC)]Cl_2$ were prepared as previously reported.[57] The macrocycle 9-[(1,4,7,10-tetraazacyclododecan-1-yl)methyl]acridine (ACR) and complex $[Zn(ACR)]Cl_2$ were prepared similarly to a previously reported procedure but using ethanolic $ZnCl_2$ instead of $Zn(ClO_4)\cdot 6H_2O$.[59] DNA oligonucleotides were purchased from Integrated DNA Technologies (IDT) in desalted form. DNA was dissolved in 100 mM KCl (G-quadruplexes) or 100 mM NaCl (duplexes). Solutions of G-quadruplex and duplex DNA were annealed by heating solutions up to

dx.doi.org/10.1021/ic501484p | Inorg. Chem. 2014, 53, 11540−11551

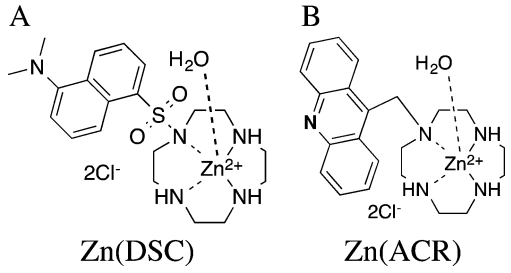

Figure 2. Zn^{2+} macrocyclic complexes.

70−75 °C for 5−10 min, followed by slow cooling (8−12 h) to room temperature. The oligonucleotide concentrations were determined by UV−vis spectroscopy at 25 °C using a molar extinction coefficient provided for each oligonucleotide at 260 nm.

General Instrumentation. ^{1}H NMR spectra were obtained on a Varian INOVA 500 MHz NMR spectrometer. Fluorescent studies were performed on a Cary Eclipse Varian fluorometer with a Varian temperature regulator. Isothermal calorimetry (ITC) data were collected on a MicroCal VP-ITC calorimeter, and data were analyzed using *Origin* software. Optical thermal melting data were collected using a Beckman Coulter DU 800 spectrometer with a Beckman Coulter high-performance temperature controller. Circular dichroism (CD) experiments were done using a Jasco PFD-350*S*/350L spectrometer and a Peltier-type FDCD attachment for temperature control.

Fluorescence Spectroscopy. The binding of Zn(DSC) to oligonucleotides was studied using a previously reported procedure,[57] with minor modifications. Stock solutions of Zn(DSC), DSC, or Zn(ACR) were prepared and standardized using UV−vis spectroscopy with molar extinction coefficients of 5558 L mol^{-1} cm^{-1} at 335 nm, 3934 L mol^{-1} cm^{-1} at 335 nm, and 9920 L mol^{-1} cm^{-1} at 362 nm, respectively. Solutions of 5 or 10 μM Zn(DSC) were typically prepared in 20 mM *N*-(2-hydroxyethyl)piperazine-*N*′-ethanesulfonic acid (HEPES; pH 7.5) and 100 mM KCl (G-quadruplexes) or 100 mM NaCl (pentanucleotides and duplexes) at 25 °C. Solutions of Zn(DSC) or DSC were excited at 335 nm, and fluorescent emission was observed from 420 to 620 nm. Solutions of Zn(ACR) were excited at 362 nm, and fluorescent emission was observed from 400 to 500 nm. Fitting of the data to binding isotherms according to eq 1 was carried out as previously described.[57]

$$[L]_B = 0.5\{K_{d(app)} + [L]_T + n[S]_T - \sqrt{(K_{d(app)} + [L]_T + n[S]_T)^2 - (4[L]_T n[S]_T)}\}$$

$$I = X_{LB}I_{LB} + X_L I_L \quad (1)$$

For our G-quadruplex binding studies, I is the fluorescence intensity, $K_{d(app)}$ is the apparent dissociation constant, and $[S]_T$ represents the total G-quadruplex concentration in solution studies.[57] $[L]_T$ is the total ligand concentration in solution. L_B represents G-quadruplex-bound Zn(DSC). X_{LB} and X_L are the mole fractions of G-quadruplex-bound Zn(DSC) and free Zn(DSC), respectively, and I_{LB} and I_L are the fluorescence emission intensities of bound Zn(DSC) and free Zn(DSC), respectively.

The binding of transition metals to the macrocycle was obtained as described above, with a few modifications. Transition-metal-ion solutions were titrated into a solution of 5 μM DSC in 20 mM HEPES (pH 7.5) and 100 mM NaCl. The quenching of fluorescence was plotted against the transition-metal concentration, and data were fit to a binding isotherm.[57] For metal-ion binding studies, I is the change in the fluorescence intensity, $K_{d(app)}$ is the apparent dissociation constant of the complex, and $[S]_T$ represents the total metal concentration in solution. $[L]_T$ is the total ligand concentrations in solution. L_B represents the metal bound to DSC. X_{LB} and X_L are the mole fractions of metal-bound DSC and free DSC, respectively, and I_{LB} and I_L are the fluorescence emission intensities of metal-bound DSC and free DSC, respectively.

NMR Spectroscopy. Lyophilized DNA pentanucleotides were suspended in 1.0 mM HEPES (pH 7.5) with either 5.0 mM NaCl or 50 mM NaCl. Samples were then lyophilized using a SpeedVac and resuspended in 99.9% D_2O three times. The concentration of the pentanucleotide samples ranged from 0.750 and 0.250 mM for NMR titration experiments. Titrations were conducted at two NaCl concentrations, 50 mM for samples containing 0.25 mM DNA or 5.0 mM for samples containing 0.75 mM DNA. Two-dimensional (2D) NMR data were collected on either a 1.5 mM or 0.75 mM DNA sample containing 5.0 mM NaCl and 1.0 mM HEPES (pH 7.5) and in D_2O.

^{1}H NMR spectra of the 0.75 and 0.25 mM pentanucleotide titrations with Zn(DSC) had 1000 transients collected for each spectrum at 25 °C. 2D NMR data were collected using a 0.75 mM DNA sample containing 5.0 mM NaCl and 1.0 mM HEPES (pH 7.5) and D_2O. NOESY and DQF-COSY data consisted of 512 free induction decay with 4K data points and 48 transients per free induction decay. The second dimension was zero-filled to 4K, and both dimensions apodized with a shifted sine-bell function. NMR spectra were then analyzed using *SPARKY NMR* analysis software.

ITC. Oligonucleotide solutions (20 μM) were prepared in 20 mM HEPES (pH 7.5) and 100 mM KCl (G-quadruplexes) or 100 mM NaCl (oligonucleotides). A solution of Zn(DSC) was prepared in double-distilled H_2O and standardized by UV−vis spectroscopy. A total of 36−38 injections were used for studies with H-Telo and 55−58 injections with pentanucleotides. Injections of 5−7 μL were made every 275−300 s at a rate of 2 s/μL to a solution of buffer or DNA, stirring at 116 rpm, at 25 °C. A blank run was also conducted under identical conditions to correct for heat signatures observed for the solvation of Zn(DSC) into the buffer. The resulting data were fit by using eqs 2 and 3, as documented in *Origin* software provided by MicroCal. The heat in microcalories per second was integrated against the blank run. The heat associated from the blank run was subtracted from that of the ligand into a solution of DNA. Two equations from this software were used to analyze the data: one-site binding and sequential binding modes. Equations 2 and 3 are given for one-site and sequential binding modes, respectively.

$$Q = n\Theta M_t \Delta H V_0$$

$$Q = \frac{nM_t\Delta HV_0}{2}\left[1 + \frac{X_t}{nM_t} + \frac{1}{nKM_t}\right] - \sqrt{\left(1 + \frac{X_t}{nM_t} + \frac{1}{nKM_t}\right)^2 - \frac{4X_t}{nM_t}} \quad (2)$$

For DNA binding studies using a single binding mode, the binding sites are considered equal. Q is the total heat content, n is the number of sites, ΔH is the molar heat of ligand binding, Θ is the fraction of sites occupied by the ligand, i is the injection number, and K is the apparent association constant. V_0 is the volume of the cell, and M_t and X_t are the bulk concentrations of DNA and the complex, respectively.

$$F_n = \frac{K_1K_2...K_n[X]^n}{P} \quad (3)$$

$$P = 1 + K_1[X] + K_1K_2[X]^2 + ... + K_1K_2...K_n[X]^n$$

$$F_1 = \frac{K_1[X]}{P}$$

$$P = 1 + K_1[X]$$

$$F_2 = \frac{K_1K_2[X]^2}{P}$$

$$P = 1 + K_1[X] + K_1K_2[X]^2$$

dx.doi.org/10.1021/ic501484p | *Inorg. Chem.* 2014, 53, 11540−11551

$$Q = M_t V_0[F_1\Delta H_1 + F_2(\Delta H_1 + \Delta H_2) + \ldots + F_n(\Delta H_1 + \Delta H_2 + \Delta H_3 + \ldots + \Delta H_n)]$$

For DNA binding studies using a sequential binding mode, the binding sites are not considered equal. All of the parameters used in eq 2 are the same as those for eq 3. F is the fraction of total macromolecules having n bound ligands.

Optical Thermal Melting. Aqueous solutions of 5 or 10 μM Zn(DSC) and 5 μM H-Telo were prepared in 20 mM HEPES (pH 7.5) and 100 mM KCl for optical thermal melting studies. Absorbance readings at 260 nm were taken every 1 min as the temperature was raised at a rate of 0.5 °C/min. Melting temperatures (T_m) were obtained by fitting of the data to the *Meltwin* 3.5 program available at http://www.meltwin3.com/.[60]

CD Spectroscopy. CD spectra of 5.0 μM G-quadruplex DNA, with up to 2 equiv of Zn(DSC), were prepared in 20 mM HEPES (pH 7.5) and 100 mM KCl in 1.0 cm cuvettes at 25 °C. Spectra were taken from 340 to 220 nm.

RESULTS

The H-Telo G-quadruplex was chosen as a well-studied example of a G-quadruplex containing several loop thymines for potential interaction with the Zn^{2+} complexes. H-Telo is known to form a 3:1 hybrid structure in the presence of K^+. Evidence supporting the formation of this structure was obtained from CD spectroscopy, which matched that of similar G-quadruplex-forming DNA sequences published previously.[8] In addition, several mutations were made in the nucleobases contained in the H-Telo G-quadruplex loops. All DNA sequences listed in Table 1 gave CD spectra that were consistent with a G-quadruplex structure, as shown by the prominent band at 290 nm with positive ellipticity.[8] Replacement of the guanosine residues with adenines in order to disrupt G-quadruplex formation gave CD spectra with no maximum at 290 nm (Figure SI-1 in the Supporting Information). The ATA-mutated G-quadruplex showed an additional shoulder at 270 nm (Figure SI-2c in the SI), which is observed in other human telomeric G-quadruplex variants.[8,11] The addition of up to 2 equiv of Zn(DSC) to any of the G-quadruplex sequences did not markedly change the CD spectra of the DNA (Figure SI-2 in the SI). Furthermore, optical thermal melting experiments showed that Zn(DSC) did not perturb the structure of native H-Telo (Figure SI-2a in the SI).

Binding of the Zn(DSC) complex to the human telomeric sequence, H-Telo, as well as to several G-quadruplex variants containing loop mutations (Figure 1) was studied by monitoring the change in fluorescence emission of the dansyl pendent group in the Zn(DSC) complex (Figure 3). The fluorescence emission of the Zn(DSC) complex at 565 nm shifted by about 25 nm upon binding to H-Telo (Figure 3A). The observed blue shift in fluorescence emission, with a concurrent increase in the fluorescence intensity, is consistent with placement of the dansyl group in a more hydrophobic environment. Binding isotherms are best fit by an equation expressing binding (eq 1) to two identical sites on H-Telo (Figure 3B, solid line) to give a K_d of 2.5 μM (Table 2). Fitting of the data to equations that specify a single binding site gave a slightly poorer fit to the isotherm with a K_d of 0.40 μM (Figure 3B, dashed line). Remarkably, binding of the Zn(DSC) complex to H-Telo was retained, although weakened, in relatively high concentrations (1.8 mM) of phosphate ($K_{d(app)}$ = 2.7 μM) for 1:1 stoichiometry or ($K_{d(app)}$ = 9.2 μM) for 2:1 stoichiometry (Figure SI-3 in the SI).

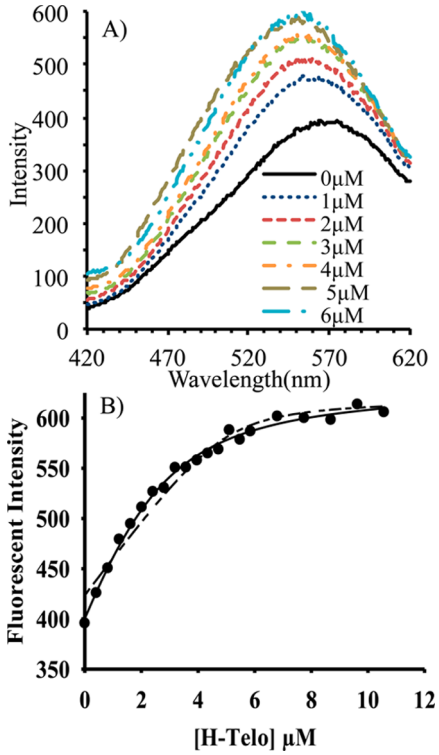

Figure 3. (A) Fluorescence emission of a solution containing 5 μM Zn(DSC) titrated with H-Telo in 100 mM KCl and 20 mM HEPES (pH 7.5) at 25 °C. (B) Binding isotherms, n = 1 ($K_{d(app)}$ = 0.4 μM; R^2 = 0.9695; dashed line) and n = 2 ($K_{d(app)}$ = 2.5 μM; R^2 = 0.9939; solid), for emission at 540 nm versus [H-Telo] as fit to eq 1.

Table 1. Apparent Dissociation Constants ($K_{d(app)} \times 10^{-6}$ M) for Transition-Metal Ions Bound to DSC and H-Telo

M^{2+}	DSC $K_{d(app)}$[a]	H-Telo $K_{d(app)}$ (n)[b]
Zn^{2+}	1.1 ± 0.2	2.5 ± 0.1 (2)
Cu^{2+}	<1	NB[c]
Fe^{2+}	weak	NB[c]
Cd^{2+}	6.7 ± 0.2	12.5 ± 2.0 (1)
Co^{2+}	49.0 ± 5.1	NB[c]

[a]Apparent dissociation constants of M(DSC) obtained from fitting of the data to eq 1 in solutions containing 100 mM NaCl and 20 mM HEPES (pH 7.5) at 25 °C. [b]Dissociation constant for binding to the H-Telo G-quadruplex in solutions containing 100 mM KCl, n = stoichiometric value (complex–DNA) from the fit of the data to eq 1. [c]NB = no measurable binding due to minimal fluorescence change.

Table 2. Apparent Dissociation Constants ($K_{d(app)} \times 10^{-6}$ M)[a] of Zn(DSC) to G-Quadruplexes

sequence	modification	$K_{d(app)}$ $(n = 2)$[b]
$A(G_3T_2A)_3G_3$	native (TTA)	2.5 ± 0.3
$A(G_3TA_2)_3G_3$	TAA	13.3 ± 0.4
$A(G_3ATA)_3G_3$	ATA	5.4 ± 0.4
$A(G_3TAT)_3G_3$	TAT	7.2 ± 0.2
$A(G_3CA_2)_3G_3$	CAA	very weak

[a]Apparent dissociation constants of Zn(DSC) (5 μM) with the G-quadruplex as determined by fitting of the data to eq 1 in solutions containing 100 mM KCl and 20 mM HEPES (pH 7.5) at 25 °C. [b]Stoichiometric value (complex–DNA, n); determined by setting n = 2 in eq 1.

dx.doi.org/10.1021/ic501484p | Inorg. Chem. 2014, 53, 11540–11551

Binding of Zn(DSC) to H-Telo is highly pH-dependent (Figure 4). $K_{d(app)}$ weakens by almost 35-fold upon a change in

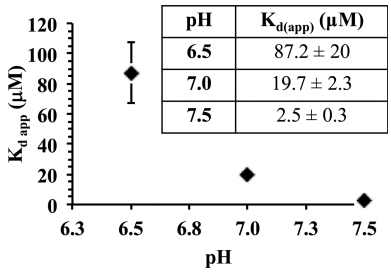

Figure 4. pH dependence of Zn(DSC) binding to H-Telo in 100 mM KCl and 20 mM HEPES. Inset: Apparent dissociation constants from fitting of the data to eq 1 (n = 2) in 100 mM KCl and 20 mM HEPES.

the pH from 6.5 to 7.5 for data fitting to a 2:1 stoichiometric ratio. This pH dependence supports binding of the Zn^{2+} center to the deprotonated N3 of the thymine nucleobase.[52,59] Other studies support the requirement of Zn^{2+} in binding. The free macrocycle, DSC, did not detectably bind to H-Telo at up to 6 equiv of DNA (Figure SI-4 in the SI). The addition of ethylenediaminetetraacetic acid (EDTA) to a solution containing Zn(DSC) adduct with H-Telo produced the fluorescence spectrum of the free DSC macrocycle nearly instantaneously (Figure SI-5 in the SI). This is consistent with the rapid equilibration of ligands with Zn^{2+} ion and G-quadruplex.

Interestingly, the H-Telo adduct with Zn(DSC) forms even if all components were added separately in solution, regardless of the order of the addition of components (Figure 5). These

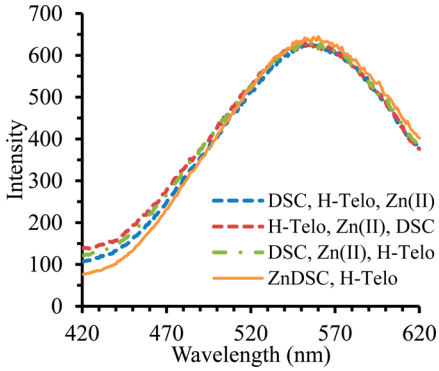

Figure 5. Self-assembly of the H-Telo–Zn(DSC) adduct. Fluorescence spectra of equimolar concentrations (5 μM) of DSC, H-Telo, and $ZnCl_2$ in 100 mM KCl and 20 mM HEPES (pH 7.5) with components added in the order listed.

results correlate with the relatively large binding constant of Zn^{2+} to the DSC macrocycle at neutral pH (Table 1 and Figure SI-6 in the SI). Such a self-assembly feature may be useful in the further development of this system as a Zn^{2+} sensor. Studies were carried out to investigate the selectivity of the G-quadruplex–DSC combination for Zn^{2+} over other metal ions.

Other first-row transition-metal ions including Cu^{2+}, Fe^{2+}, and Co^{2+} do not promote the formation of a stable adduct with H-Telo as studied by fluorescence spectroscopy (Table 1 and Figures SI-7–SI-12 in the SI). Cu^{2+} binds strongly to DSC, as shown by fluorescence titrations. However, the fluorescence emission of Cu(DSC) changes very little upon the addition of 6 equiv of H-Telo, consistent with the negligible interaction of the Cu^{2+} complex with G-quadruplex under these conditions. Co^{2+} binds DSC more weakly than Cu^{2+} or Zn^{2+}. The minimal changes in DSC fluorescence upon the addition of Co^{2+} and DSC to H-Telo are consistent with negligible adduct formation. This interaction is consistent with the relatively weak binding of Co^{2+} to DSC and H-Telo under these conditions. The binding of Fe^{2+} to the DSC macrocycle is also weak, as shown by minor changes in the fluorescence emission of DSC upon the addition of Fe^{2+}. The addition of H-Telo does not affect the fluorescence emission spectrum of solutions containing DSC and Fe^{2+}. Cd^{2+} binds more weakly to DSC than does Zn^{2+}, but the complex is nearly fully formed at 5 μM DSC and 15 μM Cd^{2+} (Figure SI-13 in the SI). The Cd(DSC) complex interacts with H-Telo ($K_{d(app)}$ = 12.5 μM), as shown by fluorescence spectroscopy. The binding isotherm for Cd(DSC) with H-Telo can be fit to a binding curve with 1:1 stoichiometry (Figure SI-14 in the SI).

In order to study the role of the loop nucleotide sequence, several mutant H-Telo G-quadruplexes with sequences of TTA, ATA, TAT, and CAA were studied with Zn(DSC) (Table 2). All G-quadruplexes that contained thymine in the loop structure bound Zn(DSC). Titration of thymine-containing mutant H-Telo G-quadruplexes into solutions containing Zn(DSC) gave binding isotherms that fit equally well to binding equations with either one or two binding sites (Figures SI-15–SI-17 in the SI). These mutants bound Zn(DSC) less tightly than did the native G-quadruplex. In contrast, fluorescence titrations were consistent with only weak interaction of the G-quadruplex which lacked thymines in loops (CAA) with Zn(DSC) (Figure SI-18 in the SI).

The binding of Zn(DSC) to short oligonucleotides containing zero, one, or two thymines was studied in order to better understand the rules for binding to loops that contain multiple thymines (Table 3). While these short oligonucleotides are simple and conformationally flexible relative to the more structurally complicated G-quadruplex structures, they are useful for studying the magnitude and stoichiometry of binding to different sequences. The fluorescence emission intensity increases as Zn(DSC) binds to thymine-containing oligonucleotides; however, the effect is not as pronounced because with the H-Telo there is no blue shift in the emission wavelength (Figures SI-19 and SI-20 in the SI). Zn(DSC) bound moderately strongly to the three oligonucleotides containing thymines but not to CCCCC.[57] Binding isotherms were fit to eq 1 for binding to a single site. Data for

Table 3. Apparent Dissociation Constants ($K_{d(app)} \times 10^{-6}$ M) of Zn^{2+} Macrocyclic Complexes with DNA

	$K_{d(app)}$ (n)[a]	
sequence	Zn(DSC)	Zn(ACR)
H-Telo	2.5 ± 0.1 (2)	1.0 ± 0.04 (5)
DD	44 ± 5 (1)	2.1 ± 0.1 (2)
CCTCC	50 ± 7 (1)[b]	5.2 ± 1.9 (1)
CTTCC	3.8 ± 0.9 (1)	1.1 ± 0.1 (2)
CTCTC	6.8 ± 0.8 (1)	1.5 ± 0.2 (2)
CCCCC	>100[b]	18

[a]Apparent dissociation constants of Zn(DSC) and DNA as determined by fitting of the data to eq 1 in 100 mM KCl (for H-Telo) or 100 mM NaCl (for oligonucleotides and duplexes) and 20 mM HEPES (pH 7.5) at 25 °C. Stoichiometric value (complex–DNA, n) determined by fitting the data to eq 1. [b]From the work reported in ref 57.

dx.doi.org/10.1021/ic501484p | Inorg. Chem. 2014, 53, 11540–11551

oligonucleotides with two thymines could equally well be fit to binding equations for two binding sites. The Dickerson dodecamer (DD), used as an example of duplex DNA, interacts with Zn(DSC) to give a moderate dissociation constant of 44 μM, when fit to binding isotherms with a single binding site (Figure SI-21 in the SI).

Zn(ACR) binding to H-Telo, short oligonucleotides, or the DD (Table 3 and Figures SI-22–SI-27 in the SI) was studied for comparison to Zn(DSC). Acridine is a strong intercalator for duplex DNA and has also been shown to stack on G-tetrads. Binding isotherms for Zn(ACR) interaction with H-Telo fit best to equations containing five binding sites and a K_d of 0.6 μM, at pH 7.5. Unlike Zn(DSC), Zn(ACR) binds to DNA with quenching of fluorescence. Strong binding of Zn(ACR) to the DD and to thymine-containing oligonucleotides was observed, giving only a 2-fold advantage to G-quadruplex DNA. In contrast to Zn(DSC) binding, Zn(ACR) showed a very weak pH dependence for binding to H-Telo (pH 6.5, 1.5 ± 0.041 μM; pH 7.5, 1.0 ± 0.04 μM for n = 5). Zn(ACR) also bound tightly to thymine-containing pentanucleotides. The binding interactions were consistently tighter than that observed with Zn(DSC). Binding isotherms are fit optimally to models with a high stoichiometric coefficient (n), consistent with binding of multiple Zn(ACR) complexes. The binding of multiple Zn(ACR) complexes is favored by stacking of acridine pendents on thymine and on each other, as reported previously.[58] Zn(ACR) bound to CCCCC as well, albeit more weakly than to the thymine-containing oligonucleotides.

The binding of Zn(DSC) to G-quadruplex DNA and to several oligonucleotides was studied by using ITC, in part to further study the stoichiometry of binding. Two different types of equations were used to fit ITC data, one with multiple equivalent binding sites (eq 2) with both $K_{d(app)}$ and n as variables and one with two binding sites of different magnitude (eq 3). ITC data fit to eq 2 is shown in Tables 4 and SI-1 in the SI and fit to eq 3 in Table SI-2 in the SI. The binding of Zn(DSC) to H-Telo was fit to an identical binding site (n) model to give a $K_{d(app)}$ of 6 μM and n = 1.7 (Figure 6). Fitting of the ITC data to a model with two binding sites of different magnitude gave dissociation constants within experimental error of each other (Table SI-2 and Figure SI-28 in the SI). These data correspond well to that obtained by fluorescence titrations. The binding constants for Zn(DSC) to CCTCC, CTTCC, and CTCTC were also determined from ITC data (Table 4 and Figures SI-29–SI-31 in the SI). Data for both CCTCC and CTTCC gave binding site stoichiometries of close to 1 when fit to eq 2, whereas fitting of the data for CTCTC gave an n value of 1.6, suggesting the binding of more than one Zn(DSC) to DNA. Consistent with this model, fitting of the data for CTTCC to eq 3 for binding sites of different strengths gave one tight and one very weak dissociation constant (10 and 410 μM) and that for CTCTC gave two dissociation constants that were more similar (8 and 39 μM). No detectable binding was observed to CCCCC upon monitoring the titration by ITC (Figure SI-32 in the SI).

Table 4. Association and Dissociation Constants from Fitting of the Isothermal Calorimetric Titration Data for Zn(DSC) Binding to DNA

oligomer	K_a (10^4 M^{-1})[a]	K_d (μM)[b]	n[a]	ΔG (kJ/mol)[c]
H-Telo	17 ± 2.3	6.0 ± 0.8	1.7 ± 0.3	−29.2 ± 0.9
CCTCC	7.5 ± 1.0	13.7 ± 2.5	1.1 ± 0.3	−27.8 ± 0.5
CTTCC	13 ± 4.7	8.0 ± 4.0	0.83 ± 0.1	−29.0 ± 1.0
CTCTC	9.9 ± 3.4	11.4 ± 4.7	1.6 ± 0.4	−28.4 ± 1.0
CCCCC		NB[d]		

[a]Apparent association constants and stochimetric values derived from fitting of the data to eq 2. Titrations had 20 μM oligonucleotide, variable Zn(DSC) concentrations, 100 mM KCl (for H-Telo) or 100 mM NaCl (for oligonucleotides and duplexes), and 20 mM HEPES (pH 7.5) at 25 °C. [b]Calculated as $1/K_a$. [c]Calculated using $\Delta G = RT(\ln K_a)$ at 25 °C. [d]No binding observed.

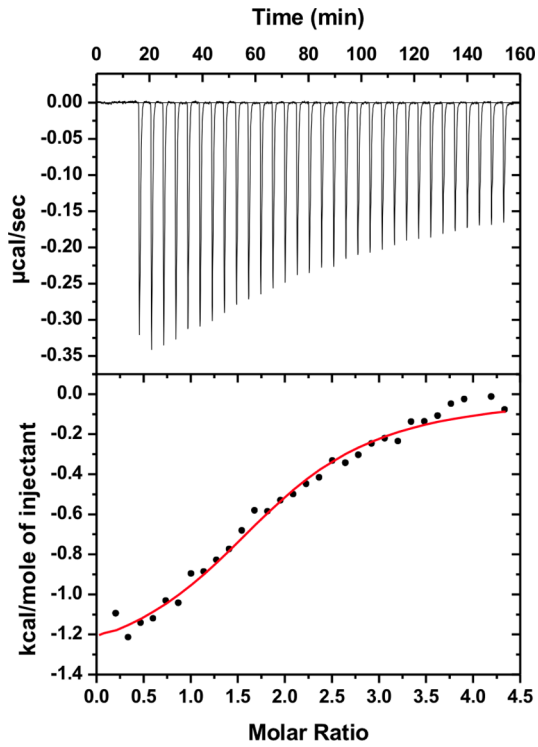

Figure 6. ITC trace of a solution of 20 μM H-Telo in 100 mM KCl and 20 mM HEPES (pH 7.5) at 25 °C. Top: Heat evolution from titration of Zn(DSC) into a H-Telo solution. Bottom: Plot of heat (kcal/mol) obtained from subtracting the integrated peak area of buffer from DNA versus molar ratio of Zn(DSC) to DNA fit to eq 2.

NMR was used to provide additional information on the binding of Zn(DSC) to DNA. Analysis of NOESY and DQF-COSY spectra provided information on the chemical shift assignments for the dansyl aromatic protons in the absence and presence of DNA. The assignments of the dansyl pendent group protons were based, in part, on the observation of NOESY cross peaks to the dansyl methyl proton resonance at 2.92 ppm (Figure SI-33 in the SI). The observed NOEs are consistent with the dansyl H1 (7.50 ppm) and H4 (8.67 ppm) protons. The DFQ-COSY correlations to these proton resonances enabled the assignment of the H2, H3, H5, and H6 protons (Figure SI-34 in the SI). A weak NOE between a proton on the cyclen ring and the H3 of the dansyl pendent ring was observed, confirming these assignments (Figure SI-34 in the SI). Due to overlapping resonances, the cyclen protons could not be unequivocally assigned.

Several oligonucleotides including CCCCC, CCTCC, CTTCC, and CTCTC were studied by ^{1}H NMR. CCCCC was used as a control sequence to identify dansyl proton resonances associated with nonspecific binding. The other oligonucleotides provided several permutations of tandem and

dx.doi.org/10.1021/ic501484p | Inorg. Chem. 2014, 53, 11540–11551

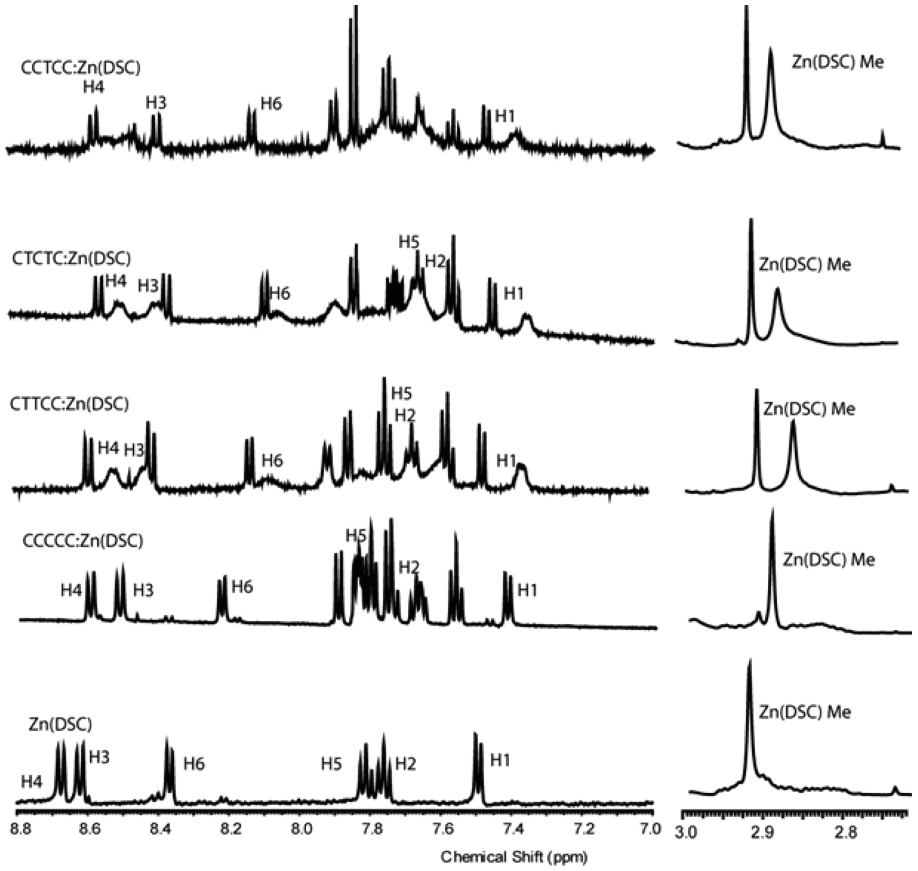

Figure 7. NMR spectra recorded at 25 °C of Zn(DSC) and the four different pentanucleotides (0.75 mM) with 1 equiv of Zn(DSC) in 5.0 mM NaCl and 0.75 mM HEPES (pH 7.5). See also Figures SI35–SI38 in the SI.

single thymines in a single-stranded oligonucleotide. Experiments were carried out initially with near-millimolar concentrations (0.75 mM) of oligonucleotide and Zn(DSC) complex and, second, with lower concentrations (0.25 mM) of DNA and Zn(DSC) complex. In experiments containing 0.75 mM concentrations of oligonucleotide, low concentrations of NaCl (5.0 mM) were necessary to avoid precipitation of the Zn(DSC)–DNA complex. Experiments performed with 0.25 mM DNA and Zn(DSC) complex contained 50 mM NaCl, to approximate conditions used for ITC and fluorescence titrations.

In NMR spectra of the Zn(DSC)–CTTCC complex at 0.75 mM with 5.0 mM NaCl, there were two distinct sets of dansyl proton resonances (Figure 7). 2D NMR experiments were used to identify the aromatic dansyl protons resonance in the Zn(DSC)–CTTCC complex (Figures SI-33 and SI-34 in the SI). The results show two distinct Zn(DSC)–oligonucleotide adducts in which one adduct has sharp, well-resolved resonances and the second has broader, less-defined resonances. Similar results were also observed for titration of Zn(DSC) into CTCTC and CCTCC (Figures SI-36 and SI-37 in the SI). The Zn(DSC)–CCCCC complex exhibited one set of well-defined and narrow resonances with ~0.1 ppm or less upfield shifts of the dansyl aromatic proton resonances, indicating potentially nonspecific binding to the CCCCC (Figure SI-38 in the SI). Table 5 provides the chemical shift assignments for the Zn(DSC) dansyl group proton resonances complexed with CTTCC and CCCCC. Given that there is no evidence of binding to the CCCCC sequence in ITC and fluorescence experiments at higher NaCl concentrations, these

Table 5. Chemical Shift Values for the Dansyl Pendent Group When Bound to CCCCC or CTTCC and Changes in the Chemical Shift (Δ ppm) from Unbound Zn(DSC)[a]

		CTTCC		
proton[b]	Zn(DSC) only	nonspecific (Δppm)[c]	T-specific (Δppm)[d]	CCCCC[c] (Δppm)
H1 (d)	7.5	7.46 (−0.04)	7.37 (−0.13)	7.48 (−0.02)
H2 (t)	7.76	7.74 (−0.02)	7.60 (−0.16)	*e*
H3 (d)	8.64	8.38 (−0.26)	8.44 (−0.20)	8.58 (−0.06)
H4 (d)	8.67	8.57 (−0.10)	8.51 (−0.16)	8.66 (−0.01)
H5 (t)	7.82	7.75 (−0.07)	7.68 (−0.014)	*e*
H6 (d)	8.36	8.1 (−0.25)	8.07 (−0.29)	8.29 (−0.07)

[a]In D_2O, 5.0 mM NaCl and 0.75 mM HEPES (pH 7.5). [b]Parentheses denote multiplet of the dansyl resonance. [c]Chemical shifts associated with sharp resonances from Figure 7 (parentheses denote the change in the chemical shift; − value indicates an upfield shift). [d]Chemical shifts associated with broad resonances from Figure 7 (parentheses denote the change in the chemical shift; − value indicates an upfield shift). [e]Not observed due overlap.

data, in particular the sharp dansyl resonances, indicate that the low-salt conditions favor nonspecific interactions between the positively charged Zn^{2+} and the phosphodiester backbone that are likely electrostatic in nature. A second NMR titration with the CCCCC pentanucleotide and Zn(DSC) at 50 mM NaCl shows that the Zn(DSC) resonances do not shift appreciably (Figure 8), consistent with the absence of any adduct formation. However, NMR titrations at these lower concentrations of CTTCC resulted in a predominant set of peaks that

dx.doi.org/10.1021/ic501484p | *Inorg. Chem.* 2014, 53, 11540–11551

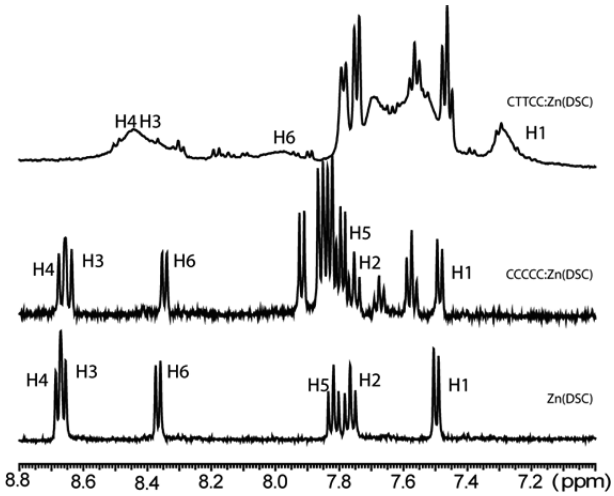

Figure 8. ^{1}H NMR spectra recorded at 25 °C of Zn(DSC) and CCCCC and CTTCC with 0.25 mM of each in 50 mM NaCl and 0.75 mM HEPES (pH 7.5).

exhibited line broadening that precluded further experiments under these conditions.

Further analysis of the NMR chemical shift data for CCCCC and CTTCC at 0.75 mM DNA shows that the H1, H2, H4, and H6 resonances for the Zn(DSC) adduct with CTTCC exhibited chemical shift differences larger than those of Zn(DSC) with CCCCC (Table 5). In contrast, the chemical shift differences for the H3 and H5 dansyl protons corresponding to the thymine-specific adduct were less than those corresponding to the nonspecific CCCCC adduct. When stacked on a thymine, the H1, H2, H4, and H6 dansyl protons would most likely be shielded more by the thymine aromatic ring, while the H5 and H3 protons would extend beyond the edge of thymine and thus would exhibit a smaller upfield shift. In addition, the CTTCC, CTCTC, and CCTCC thymine H6 and methyl protons broaden in the presence of Zn(DSC), indicating that the Zn(DSC) dansyl pendent interacts with thymine and most likely is stacked on the thymine base.

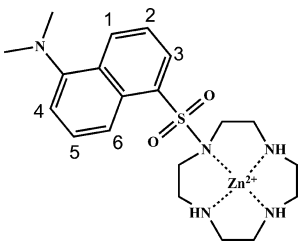

DISCUSSION

Binding Selectivity of Zn^{2+} Complexes to G-Quadruplexes. Our interest in the development of Zn^{2+} complexes that bind specifically to thymine-containing loops in G-quadruplexes led us to consider the H-Telo G-quadruplex. H-Telo is a well-studied sequence in the human genome that forms a G-quadruplex with three loops containing two thymines each. In solutions containing 100 mM KCl, H-Telo forms the 3 + 1 hybrid structure, which contains two lateral loops connecting the tetrads and one propeller loop. The thymines in the lateral G-quadruplex loops have exposed Watson−Crick faces that are accessible for binding of the Zn^{2+} centers.[9,10] Two Zn^{2+} complexes, Zn(DSC) and Zn(ACR), were chosen to study binding to H-Telo and related mutant derivatives of the H-Telo G-quadruplex, with the goal of studying the effect of the two very different pendent groups on G-quadruplex binding and selectivity. The dansyl group of Zn(DSC) is not planar and contains a bulky dimethylamine substituent. By contrast, acridine of Zn(ACR) is a planar intercalator that may stack on thymine. The fluorescent properties of the acridine and dansyl pendent groups are suitable for direct fluorescent monitoring of the binding of the complexes to DNA. Both complexes have been shown to bind to thymine-containing DNA in single-stranded form.[54,58]

The Zn(DSC) complex binds tightly to the H-Telo G-quadruplex with dissociation constants in the low micromolar range for a 2:1 binding model as supported by both fluorescence and ITC titrations. Both the fluorescence spectroscopy and ITC data can be fit to binding isotherms to give similar binding constants of 2.4 μM (n = 2) and 6.0 μM (n = 1.7), respectively. Alternatively, the ITC data can be fit to a binding isotherm with two different sites to give two K_d values that are, nonetheless, similar in magnitude (6.3 ± 5.6 and 13.6 ± 4.6 μM). That the two sites have similar binding constants suggests that the two Zn(DSC) complexes bind to H-Telo independently and do not influence each other when binding. Given that there are two thymines in each of the three loops, this might involve binding of consecutive thymines in the same loop or in different loops. The fact that binding of the two Zn(DSC) complexes to H-Telo does not affect each other is most consistent with binding to two different loops. Characterization of Zn(DSC) binding to pentanucleotides using ITC and fluorescence titrations as discussed further below is consistent with this interpretation. The interaction between Zn(DSC) and H-Telo is selective because of the nature of the thymines in the G-quadruplex. The exposed Watson−Crick faces allow for coordination of the Zn^{2+} center to the N3 of thymine. This interaction produces 110-fold selectivity of Zn(DSC) to a thymine in the H-Telo loop compared to duplex DNA. Other pertinent data include a 35-fold increase in the binding strength with increasing pH over the range of 6.5−7.5, which is consistent with the importance of the Zn^{2+} center interaction with the thymine residues found in the G-quadruplex loop.[52,59] Furthermore, Zn(DSC) shows a large increase in the fluorescence intensity with a concurrent shift in the emission wavelength, consistent with the dansyl fluorophore being in a more hydrophobic medium as it binds to H-Telo.

The binding selectivity of Zn(DSC) to H-Telo in comparison to duplex DNA is similar in magnitude to that reported for other G-quadruplex binders.[19] Assessment of the G-quadruplex selectivity is made more difficult by the apparent multiple binding sites for Zn(DSC) complexes on G-quadruplex in comparison to the DD, the duplex DNA used in this study. If the dissociation constant for the 1:1 stoichiometry for the H-Telo−Zn(DSC) adduct is compared to a 1:1 dissociation constant for DD−Zn(DSC), the selectivity for the G-quadruplex is 110-fold. A comparison of the 2:1 dissociation constant for H-Telo−Zn(DSC) to the 1:1 ratio for the DD−Zn(DSC) gives a 20-fold ratio in the magnitude of the dissociation constants. However, the 2:1 stoichiometric ratio dictates that there are twice as many binding sites for Zn(DSC) on H-Telo as on DD, which would double the amount of bound Zn(DSC) relative to DNA with a single binding site. Thus, the stiochiometric ratio factors into the G-quadruplex selectivity.

dx.doi.org/10.1021/ic501484p | Inorg. Chem. 2014, 53, 11540−11551

Loop mutants with different sequences containing one or two thymines were studied in an attempt to parse the sequence dependence of binding. CD spectra of the mutants, with the exception of the ATA mutant, were very similar to that of the native H-Telo, allowing for their comparison in a structural context. The CD spectrum of the ATA mutant has a barely discernible shoulder at 270 nm, while all other mutant G-quadruplex CD spectra are similar to that of the native. Notably, the shoulder observed at 270 nm of ATA is also observed in several other H-Telo models, suggesting that the ATA mutant forms the 3 + 1 structure.[8,11] The binding of Zn(DSC) to these mutants was determined assuming a binding mode similar to that obtained with H-Telo (n = 2). Overall, the mutant G-quadruplexes containing thymine in loops bound Zn(DSC) more weakly than the native. The G-quadruplex with CAA loops bound Zn(DSC) very weakly. Nearly equivalent $K_{d(app)}$ values, obtained via fluorescence titrations, for the mutant H-Telo derivatives suggest that Zn(DSC) does not have a large preference for thymine residues in different positions of the H-Telo loops.

To further study the effect of tandem thymine groups versus ones that have intervening nucleotides, CTTCC, CTCTC, and CCTCC, were studied. Notably, changes in the Zn(DSC) fluorescence spectrum are not as pronounced as those with H-Telo. This is most likely due to the decreased hydrophobic surface area of pentanucleotides and the absence of a cavity formed by the G-quadruplex that creates a unique environment. Fluorescence titrations and ITC data show that Zn(DSC) binds most tightly to pentanucleotides containing multiple thymines. A single thymine in CCTCC gave a moderate dissociation constant of 50 or 14 μM by fluorescence spectroscopy[57] and ITC, respectively, for a data fit to a single-site binding equation. Pentanucleotides containing adjacent thymines (CTTCC) or with a cytosine spacer (CTCTC) bound more tightly to Zn(DSC) than did the oligonucleotide containing a single thymine when fluorescence data were fit to a 1:1 binding model (Table 3). Fitting of the data to binding isotherms with a 2:1 stoichiometry gave no improvement over fitting to isotherms with a 1:1 ratio of Zn(DSC) to DNA. The sequence containing tandem thymines (CTTCC) indeed showed strong binding of only a single Zn(DSC) complex, as shown by fitting of the ITC data using either identical or sequential binding sites. This suggests that the close proximity of the two thymines precludes tight binding of two adjacent Zn(DSC) complexes. In contrast, ITC data for CTCTC were consistent with the binding of more than one Zn(DSC) complex. Relatively similar binding constants were obtained using eq 3 for multisite binding and a stoichiometric factor of 1.6 using eq 2. This supports binding of multiple Zn(DSC) to CTCTC, where the cytosine spacer allows for the binding of Zn(DSC) to both thymines. These binding preferences obtained for Zn(DSC) with pentanucleotides are informative for understanding the binding mode of Zn(DSC) to H-Telo. The fact that Zn(DSC) complexes do not bind strongly to tandem thymines supports our hypothesis that the two H-Telo binding sites are on different thymines in two of the loops.

Zn(ACR) binding to H-Telo is exceptionally strong with data best fit by a 5:1 complex to H-Telo stoichiometry. These binding constants are most likely lower limits on the true dissociation constant for Zn(ACR) to the G-quadruplex, which cannot be determined accurately at the concentrations required for the fluorescence measurements. Unfortunately, the selectivity for the G-quadruplex over duplex DNA is low. The acridine pendent is a good intercalator for DNA,[61] and domination of the aromatic pendent group interactions of the complex with DNA is the likely cause of the promiscuity. The predominant influence of the acridine pendent on the binding mode is supported by the weak pH dependence of Zn(ACR) binding to H-Telo, which changes by only 1.5-fold for measurements at pH 6.5 compared to those at pH 7.5. The binding to Zn(DSC) is more pH-dependent, signaling the importance of the Zn^{2+} center for Zn(DSC) and the lack of importance of the Zn^{2+} center for Zn(ACR). The low binding selectivity of the Zn(ACR) complex for the G-quadruplex over duplex DNA discouraged us from further experiments using this complex. Interestingly, previously studied G-quadruplex ligands that use a trisubstituted acridine as a scaffold are more selective binders.[15,22,24,62]

Zn(ACR) also binds more tightly and with less specificity than does Zn(DSC) to the pentanucleotides. In the case of CTTCC and CTCTC, Zn(ACR) binds in a 2:1 ratio. A 1:1 stoichiometric ratio provides a poorer fit, suggesting that Zn(ACR) binds to both available thymines; a similar interaction was observed for binding to thymidylylthymidine (TpT).[58] For the dinucleotide, the two Zn(ACR) complexes were proposed to bind to both thymines, with the two acridine pendents stacked on each other. This is consistent with the large aromatic surface area of the Zn(ACR) pendent having improved stacking interactions. An increase in the planar surface area also correlates to tighter nonspecific binding to the nonthymine-containing pentanucleotide (CCCCC).

NMR Titrations. ^{1}H NMR data for CTCTC, CCTCC, and CCCCC support interaction of the Zn(DSC) complex with single-stranded thymine groups. Two sets of data were collected: one set at 0.75 mM pentanucleotide, 0.75 mM Zn(DSC), and 5.0 mM NaCl and a second set at 0.25 mM pentanucleotide, 0.25 mM Zn(DSC), and 50 mM NaCl. The low salt concentrations were necessitated by the solubility of Zn(DSC), which decreases with increasing salt concentration. The results obtained from experiments using higher salt concentrations (50 mM) and lower DNA and Zn^{2+} complex concentrations agree with those obtained by using fluorescence and ITC titrations that show thymine-selective binding. The broad resonance obtained as CTTCC is added to Zn(DSC) at 50 mM salt concentration is consistent with previous observations where the aromatic pendent interacts with thymine.[56] The upfield shifts of the H6 and H3 resonances and the broadening of the thymine methyl and H6 resonances are consistent with stacking of the dansyl group on thymine. In comparison, the dansyl proton resonances do not broaden or shift as CCCCC is added to Zn(DSC). The lack of an effect on the proton resonances supports a weak interaction, as shown also by the ITC and fluorescence spectroscopy data.

A separate set of experiments was conducted using higher Zn(DSC) and oligonucleotide concentrations to assign the resonances using 2D NMR techniques. Because of the poor solubility of Zn(DSC), these experiments required 10-fold lower salt concentrations (5 mM). As Zn(DSC) was added to solutions of CCTCC, CTTCC, and CTCTC, each spectrum showed two sets of DSC group proton resonances, which were assigned to two different Zn(DSC) pentanucleotide adducts. The two separate sets of peaks are likely due to two types of DNA adducts, termed here as nonspecific and specific. The nonspecific set of resonances is likely a result of electrostatic interactions, while the specific set is consistent with the Zn^{2+} complex forming a coordination bond with the N3 of thymine.

In the case of CCCCC, however, one dominant set of sharp resonances is observed, and these are less upfield-shifted than the broad resonances. This observation, in addition to consideration of weak fluorescent and heat changes in ITC measurements, suggests that Zn(DSC) interacts weakly with CCCCC even at higher concentrations of DNA and the complex.

Binding Mode of Zn(DSC) to Noncanonical Thymines. Zn(DSC) was previously studied as a recognition agent for DNA thymine bulges. Zn(DSC) bound very weakly to the thymine bulge compared to analogous complexes with a more planar aromatic group.[57] It was postulated that Zn(DSC) was a weak binder for the extrahelical thymine bulge because of the bulky nature of the fluorophore. By contrast, the N3 of thymine residues of the G-quadruplex loops are readily available for binding compared to the binding pocket that is formed between the thymine bulge and the remainder of the bulge stem.[56] The most likely reason why the dansyl does not bind well to single thymine bulges is due to steric interactions involving the dansyl's dimethylamine group and the adjacent nucleotides and base pairs in the duplex. The structure of a bulged thymine (PDB 2LOA) with a Zn^{2+} macrocycle containing a quinolone pendent group has the quinoline stacking on the thymine with few steric interactions with the adjacent nucleotides.[57] Substituting a dansyl for the quinoline pendent group would place the bulky dimethylamino group into the major groove, creating significant steric interactions with the base pairs on either side of the bulged thymine, thus making binding less favorable. Zn(DSC), however, binds tightly to thymines in single-stranded DNA and to thymines in abasic sites, indicating higher specificity for thymines located in structures that can accommodate the dimethylamino group.[51,57] In thymine-containing hairpin loops, the nucleotides near the 180° turn in the loop could present favorable binding sites and the nucleotides in single-stranded oligonucleotides have sufficient flexibility to allow thymine to bind Zn(DSC).[63] This information can be used to rationalize the binding of Zn(DSC) to H-Telo. H-Telo G-quadruplex has six thymines but exhibits only a 2:1 Zn(DSC)−DNA stoichiometry based on fluorescence and ITC experiments. Analysis of the NMR structure of the H-Telo structure (PDB 2GKU) proposed by Patel in 2006[9] shows that T18 and T12 in this structure have the correct position and orientation to effectively bind Zn(DSC) with minimal steric interactions involving the dimethylamino group. Thymines T19 and T6 could also bind Zn(DSC), but the loop structures would have to undergo significant changes to accommodate Zn(DSC). To visualize what Zn(DSC) would look like bound to H-Telo, Zn(DSC) was visually docked on the T12 and T18 nucleotides in a way that satisfies the chemical shift differences observed in the NMR titrations and to accommodate the dansyl's dimethylamino group (Figure 9).

Role of Zn^{2+} versus Other Metal Ions. Quite remarkably, several other divalent metal ions cannot substitute for Zn^{2+}. It was especially surprising that Cu(DSC) did not measurably interact with H-Telo. The DSC macrocycle binds Cu^{2+} more tightly than Zn^{2+}, and Cu^{2+} is generally a stronger Lewis acid than Zn^{2+}. However, the pK_a value of the bound water in Cu(cyclen)(OH_2) (pK_a = 12.9)[64] is quite high in comparison to that of Zn(cyclen)(OH_2) (pK_a = 8),[45] suggesting that the Cu^{2+} complex has low Lewis acidity and thus does not coordinate to the deprotonated N3 of thymine. Notably, the magnitude of the binding interaction of the Zn^{2+} macrocyclic complex with the deprotonated N3 of uridine correlates with that of hydroxide binding.[52] Neither Co^{2+} nor Fe^{2+} bind sufficiently tightly to DSC at low micromolar concentrations to form a ternary complex with H-Telo. Cd^{2+} binds moderately strong to DSC and binds weakly to H-Telo. This is consistent with the weaker Lewis acidity of Cd^{2+} complexes in comparison to those of Zn^{2+}.[64,65] Thus, the coordination chemistry of Zn^{2+} alone is optimal for these interactions.

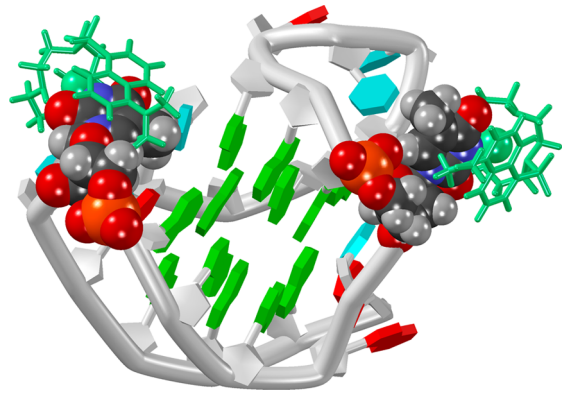

Figure 9. Model of two Zn(DSC) complexes (light green) bound to the externally positioned T18 and T12 nucleotides of the H-Telo G-quadruplex (PDB 2GKU).[9]

The Zn(DSC)−H-Telo adduct self-assembles from its independent components. Nearly identical fluorescence spectra are obtained as equimolar concentrations of Zn^{2+}, H-Telo, and DSC are added, regardless of the order of addition. The assembly of the interaction is reversible given that equimolar EDTA removes Zn^{2+} and destroys the adduct. These data imply that G-quadruplex DNA and fluorescent macrocyclic ligands might be useful as turn-on Zn^{2+}-ion sensors. The Zn^{2+} ion as a labile metal ion reversibly forms covalent bonds to both the ligand and G-quadruplex. G-quadruplex binding has been used previously to sense metal ions, including potassium or mercury, in the presence of a G-quadruplex interactive dye.[41−43] Other sensors have involved modified nucleic acid bases to detect metal ions.[66−68] The approach here is unique in that it involves using a macrocyclic ligand and a native G-quadruplex to sense Zn^{2+}.

CONCLUSIONS

Bifunctional Zn^{2+} macrocyclic complexes with pendent aromatic groups provide a useful platform for the design of recognition agents for G-quadruplexes. The Zn^{2+} complex with the nonplanar dansyl group pendent, Zn(DSC), shows moderate selectivity in binding to H-Telo over duplex DNA. The 110-fold selectivity of this complex for G-quadruplex over duplex DNA is comparable to or better than that of other reported G-quadruplex ligands. Binding studies are consistent with interaction of Zn(DSC) with thymines in two different loops in the H-Telo G-quadruplex. To the best of our knowledge, Zn(DSC) is the first coordination complex to bind tightly and selectively to H-Telo by utilizing the thymine residues as the primary mode of recognition. Organic recognition agents have been shown to interact with the nucleotides in the loops of H-Telo, but these interactions were largely secondary and driven through aromatic stacking.[23,69] The acridine-containing complex, Zn(ACR), shows tighter binding to the G-quadruplex but poor selectivity over duplex DNA.

dx.doi.org/10.1021/ic501484p | Inorg. Chem. 2014, 53, 11540−11551

The structures of G-quadruplexes are quite diverse in that loop sequences and orientation of the loops relative to the G-tetrad vary substantially.[5,70] For example, there are G-quadruplexes that have no thymines in the loops.[71] Some G-quadruplexes have single-thymine loops or multiple thymines in six nucleotide loops.[72] These loops may be lateral, diagonal, or propeller according to their position with respect to the G-tetrads.[10] Our modeling studies are consistent with the Zn(DSC) complex binding to the thymines in the two lateral loops of H-Telo, which tend to have structurally flexible regions (Figure 9). In contrast, the Zn(ACR) complex may bind to tandem thymines as shown by studies with the oligonucleotides and earlier by Kimura and co-workers.[58] Zn(ACR) has five binding sites in H-Telo, consistent with the binding of all thymines in each of the lateral loops (n = 5) in addition to binding by stacking on the G-tetrad. Future work will examine the selectivity of Zn(DSC) or Zn(ACR) as well as other Zn^{2+} complexes for binding to G-quadruplexes that contain thymines in different types of loops.

The self-assembly of the Zn(DSC) adduct with the G-quadruplex upon sequential addition of a fluorescent macrocycle, $ZnCl_2$, and H-Telo leads to an increase and shift in the fluorescence emission spectrum. The self-assembly feature may be exploited for the further development of G-quadruplex/fluorescent ligand combinations as Zn^{2+} sensors. The promise of this approach is supported by the absence of adduct formation in the presence of other biologically relevant metal ions including Fe^{2+}, Co^{2+}, and Cu^{2+}. The coordination chemistry of Zn^{2+}, which is surprisingly unique in this respect in comparison to its congeners in the periodic chart, may lead to new opportunities for the identification of Zn^{2+} ions in biological milieu.

■ ASSOCIATED CONTENT

Supporting Information

Fluorescence titrations, CD, optical thermal melting, isothermal calorimetric parameters, and NMR spectra. This material is available free of charge via the Internet at http://pubs.acs.org.

■ AUTHOR INFORMATION

Corresponding Authors

*E-mail: matthew.fountain@fredonia.edu. Tel: 716-673-3287.
*E-mail: jmorrow@buffalo.edu. Tel: 716-645- 4187. Fax: 716-645-6963.

Notes

The authors declare no competing financial interest.

■ ACKNOWLEDGMENTS

We gratefully acknowledge the National Science Foundation (Grant CHE-0911375) for support of this work.

■ REFERENCES

(1) Georgiades, S. N.; Abd Karim, N. H.; Suntharalingam, K.; Vilar, R. *Angew. Chem., Int. Ed.* **2010**, *49*, 4020−4034.
(2) Komor, A. C.; Barton, J. K. *Chem. Commun.* **2013**, *49*, 3617−3630.
(3) Keene, F. R.; Smith, J. A.; Collins, J. G. *Coord. Chem. Rev.* **2009**, *253*, 2021−2035.
(4) Neidle, S.; Balasubramanian, S. *Quadruplex nucleic acids*; RSC Publishing: Cambridge, U.K., 2006.
(5) Ou, T. M.; Lu, Y. J.; Tan, J. H.; Huang, Z. S.; Wong, K. Y.; Gu, L. Q. *ChemMedChem* **2008**, *3*, 690−713.
(6) Balasubramanian, S.; Neidle, S. *Curr. Opin. Chem. Biol.* **2009**, *13*, 345−353.
(7) Ralph, S. F. *Curr. Top. Med. Chem.* **2011**, *11*, 572−590.
(8) Ambrus, A.; Chen, D.; Dai, J.; Bialis, T.; Jones, R. A.; Yang, D. *Nucleic Acids Res.* **2006**, *34*, 2723−2735.
(9) Luu, K. N.; Phan, A. T.; Kuryavyi, V.; Lacroix, L.; Patel, D. J. *J. Am. Chem. Soc.* **2006**, *128*, 9963−9970.
(10) Burge, S.; Parkinson, G. N.; Hazel, P.; Todd, A. K.; Neidle, S. *Nucleic Acids Res.* **2006**, *34*, 5402−5415.
(11) Renciuk, D.; Kejnovska, I.; Skolakova, P.; Bednarova, K.; Motlova, J.; Vorlickova, M. *Nucleic Acids Res.* **2009**, *37*, 6625−6634.
(12) Heddi, B.; Phan, A. T. *J. Am. Chem. Soc.* **2011**, *133*, 9824−9833.
(13) Hahn, W. C. *Curr. Mol. Med.* **2005**, *5*, 227−231.
(14) Shay, J. W.; Bacchetti, S. *Eur. J. Cancer* **1997**, *33*, 787−791.
(15) Harrison, R. J.; Gowan, S. M.; Kelland, L. R.; Neidle, S. *Bioorg. Med. Chem. Lett.* **1999**, *9*, 2463−2468.
(16) Read, M. A.; Wood, A. A.; Harrison, J. R.; Gowan, S. M.; Kelland, L. R.; Dosanjh, H. S.; Neidle, S. *J. Med. Chem.* **1999**, *42*, 4538−4546.
(17) Koeppel, F.; Riou, J.-F.; Laoui, A.; Mailliet, P.; Arimondo, P. B.; Labit, D.; Petitgenet, O.; Hélène, C.; Mergny, J.-L. *Nucleic Acids Res.* **2001**, *29*, 1087−1096.
(18) Granotier, C.; Pennarun, G.; Riou, L.; Hoffschir, F.; Gauthier, L. R.; De Cian, A.; Gomez, D.; Mandine, E.; Riou, J.-F.; Mergny, J.-L.; Mailliet, P.; Dutrillaux, B.; Boussin, F. D. *Nucleic Acids Res.* **2005**, *33*, 4182−4190.
(19) White, E. W.; Tanious, F.; Ismail, M. A.; Reszka, A. P.; Neidle, S.; Boykin, D. W.; Wilson, W. D. *Biophys. Chem.* **2007**, *126*, 140−153.
(20) Tan, J. H.; Ou, T. M.; Hou, J. Q.; Lu, Y. J.; Huang, S. L.; Luo, H. B.; Wu, J. T.; Huang, Z. S.; Wong, K. Y.; Gu, L. Q. *J. Med. Chem.* **2009**, *52*, 2825−2835.
(21) Neidle, S. *Curr. Opin. Struct. Biol.* **2009**, *19*, 239−250.
(22) Campbell, N. H.; Parkinson, G. N.; Reszka, A. P.; Neidle, S. *J. Am. Chem. Soc.* **2008**, *130*, 6722−6724.
(23) Campbell, N. H.; Patel, M.; Tofa, A. B.; Ghosh, R.; Parkinson, G. N.; Neidle, S. *Biochemistry* **2009**, *48*, 1675−1680.
(24) Burger, A. M.; Dai, F.; Schultes, C. M.; Reszka, A. P.; Moore, M. J.; Double, J. A.; Neidle, S. *Cancer Res.* **2005**, *65*, 1489−1496.
(25) Gunaratnam, M.; Greciano, O.; Martins, C.; Reszka, A. P.; Schultes, C. M.; Morjani, H.; Riou, J.-F.; Neidle, S. *Biochem. Pharmacol.* **2007**, *74*, 679−689.
(26) Shin-ya, K.; Wierzba, K.; Matsuo, K.-i.; Ohtani, T.; Yamada, Y.; Furihata, K.; Hayakawa, Y.; Seto, H. *J. Am. Chem. Soc.* **2001**, *123*, 1262−1263.
(27) Kim, M.-Y.; Gleason-Guzman, M.; Izbicka, E.; Nishioka, D.; Hurley, L. H. *Cancer Res.* **2003**, *63*, 3247−3256.
(28) Kim, M.-Y.; Vankayalapati, H.; Shin-ya, K.; Wierzba, K.; Hurley, L. H. *J. Am. Chem. Soc.* **2002**, *124*, 2098−2099.
(29) Rezler, E. M.; Seenisamy, J.; Bashyam, S.; Kim, M.-Y.; White, E.; Wilson, W. D.; Hurley, L. H. *J. Am. Chem. Soc.* **2005**, *127*, 9439−9447.
(30) Izbicka, E.; Wheelhouse, R. T.; Raymond, E.; Davidson, K. K.; Lawrence, R. A.; Sun, D.; Windle, B. E.; Hurley, L. H.; Von Hoff, D. D. *Cancer Res.* **1999**, *59*, 639−644.
(31) Parkinson, G. N.; Ghosh, R.; Neidle, S. *Biochemistry* **2007**, *46*, 2390−2397.
(32) Dixon, I. M.; Lopez, F.; Tejera, A. M.; Estève, J.-P.; Blasco, M. A.; Pratviel, G.; Meunier, B. *J. Am. Chem. Soc.* **2007**, *129*, 1502−1503.
(33) Romera, C.; Bombarde, O.; Bonnet, R.; Gomez, D.; Dumy, P.; Calsou, P.; Gwan, J.-F.; Lin, J.-H.; Defrancq, E.; Pratviel, G. *Biochimie* **2011**, *93*, 1310−1317.
(34) Reed, J. E.; Arnal, A. A.; Neidle, S.; Vilar, R. *J. Am. Chem. Soc.* **2006**, *128*, 5992−5993.
(35) Bianco, S.; Musetti, C.; Krapcho, A. P.; Palumbo, M.; Sissi, C. *Chem. Commun.* **2013**, *49*, 8057−8059.
(36) Bianco, S.; Musetti, C.; Waldeck, A.; Sparapani, S.; Seitz, J. D.; Krapcho, A. P.; Palumbo, M.; Sissi, C. *Dalton Trans.* **2010**, *39*, 5833−5841.
(37) Bertrand, H.; Monchaud, D.; De Cian, A.; Guillot, R.; Mergny, J.-L.; Teulade-Fichou, M.-P. *Org. Biomol. Chem.* **2007**, *5*, 2555−2559.

(38) Arola-Arnal, A.; Benet-Buchholz, J.; Neidle, S.; Vilar, R. *Inorg. Chem.* **2008**, *47*, 11910−11919.
(39) Largy, E.; Hamon, F.; Rosu, F.; Gabelica, V.; De Pauw, E.; Guédin, A.; Mergny, J.-L.; Teulade-Fichou, M.-P. *Chem.—Eur. J.* **2011**, *17*, 13274−13283.
(40) Ma, D.-L.; Che, C.-M.; Yan, S.-C. *J. Am. Chem. Soc.* **2008**, *131*, 1835−1846.
(41) Liu, L.; Shao, Y.; Peng, J.; Huang, C.; Liu, H.; Zhang, L. *Anal. Chem.* **2014**, *86*, 1622−1631.
(42) Qin, H.; Ren, J.; Wang, J.; Luedtke, N. W.; Wang, E. *Anal. Chem.* **2010**, *82*, 8356−8360.
(43) Ge, J.; Li, X.-P.; Jiang, J.-H.; Yu, R.-Q. *Talanta* **2014**, *122*, 85−90.
(44) Ruttkay-Nedecky, B.; Kudr, J.; Nejdl, L.; Maskova, D.; Kizek, R.; Adam, V. *Molecules* **2013**, *18*, 14760−14779.
(45) Aoki, S.; Kimura, E. *Chem. Rev.* **2004**, *104*, 769−787.
(46) Shionoya, M.; Kimura, E.; Shiro, M. *J. Am. Chem. Soc.* **1993**, *115*, 6730−6737.
(47) Siters, K. E.; Sander, S. A.; Morrow, J. R. In *Progress in Inorganic Chemistry*; John Wiley & Sons, Inc.: New York, 2014; Vol. *59*; p 245.
(48) Kimura, E.; Ikeda, T.; Aoki, S.; Shionoya, M. *J. Biol. Inorg. Chem.* **1998**, *3*, 259−267.
(49) Kikuta, E.; Murata, M.; Katsube, N.; Koike, T.; Kimura, E. *J. Am. Chem. Soc.* **1999**, *121*, 5426−5436.
(50) Kikuta, E.; Katsube, N.; Kimura, E. *J. Biol. Inorg. Chem.* **1999**, *4*, 431−440.
(51) O'Neil, L. L.; Wiest, O. *J. Am. Chem. Soc.* **2005**, *127*, 16800−16801.
(52) Rossiter, C. S.; Mathews, R. A.; Morrow, J. R. *Inorg. Chem.* **2005**, *44*, 9397−9404.
(53) Wang, Q.; Lönnberg, H. *J. Am. Chem. Soc.* **2006**, *128*, 10716−10728.
(54) O'Neil, L. L.; Wiest, O. *Org. Biomol. Chem.* **2008**, *6*, 485−492.
(55) Laine, M.; Ketomaki, K.; Poijarvi-Virta, P.; Lonnberg, H. *Org. Biomol. Chem.* **2009**, *7*, 2780−2787.
(56) del Mundo, I. M. A.; Fountain, M. A.; Morrow, J. R. *Chem. Commun.* **2011**, *47*, 8566−8568.
(57) del Mundo, I. M. A.; Siters, K. E.; Fountain, M. A.; Morrow, J. R. *Inorg. Chem.* **2012**, *51*, 5444−5457.
(58) Kimura, E.; Kitamura, H.; Ohtani, K.; Koike, T. *J. Am. Chem. Soc.* **2000**, *122*, 4668−4677.
(59) Shionoya, M.; Ikeda, T.; Kimura, E.; Shiro, M. *J. Am. Chem. Soc.* **1994**, *116*, 3848−3859.
(60) McDowell, J. A.; Turner, D. H. *Biochemistry* **1996**, *35*, 14077−14089.
(61) Moloney, G.; Kelly, D.; Mack, P. *Molecules* **2001**, *6*, 230−243.
(62) Moore, M. J. B.; Schultes, C. M.; Cuesta, J.; Cuenca, F.; Gunaratnam, M.; Tanious, F. A.; Wilson, W. D.; Neidle, S. *J. Med. Chem.* **2005**, *49*, 582−599.
(63) Hare, D. R.; Reid, B. R. *Biochemistry* **1986**, *25*, 5341−5350.
(64) Kruppa, M.; Frank, D.; Leffler-Schuster, H.; König, B. *Inorg. Chim. Acta* **2006**, *359*, 1159−1168.
(65) Iranzo, O.; Richard, J. P.; Morrow, J. R. *Inorg. Chem.* **2004**, *43*, 1743−1750.
(66) Tan, S. S.; Teo, Y. N.; Kool, E. T. *Org. Lett.* **2010**, *12*, 4820−4823.
(67) Tan, S. S.; Kim, S. J.; Kool, E. T. *J. Am. Chem. Soc.* **2011**, *133*, 2664−2671.
(68) Omumi, A.; McLaughlin, C. K.; Ben-Israel, D.; Manderville, R. A. *J. Phys. Chem. B* **2012**, *116*, 6158−6165.
(69) Doria, F.; Nadai, M.; Folini, M.; Scalabrin, M.; Germani, L.; Sattin, G.; Mella, M.; Palumbo, M.; Zaffaroni, N.; Fabris, D.; Freccero, M.; Richter, S. N. *Chem.—Eur. J.* **2013**, *19*, 78−81.
(70) Balasubramanian, S.; Hurley, L. H.; Neidle, S. *Nat. Rev. Drug Discovery* **2011**, *10*, 261−275.
(71) Dexheimer, T. S.; Sun, D.; Hurley, L. H. *J. Am. Chem. Soc.* **2006**, *128*, 5404−5415.
(72) Phan, A. T.; Modi, Y. S.; Patel, D. J. *J. Am. Chem. Soc.* **2004**, *126*, 8710−8716.